CERN/LHCC 2000-011
Status Report/RD42
January 7, 2000

Development of Diamond Tracking Detectors for High Luminosity Experiments at the LHC

The RD42 Collaboration

W. Adam[1], E. Berdermann[2], P. Bergonzo[3], G. Bertuccio[4], F. Bogani[5], E. Borchi[6], A. Brambilla[3], M. Bruzzi[6], C. Colledani[7], J. Conway[8], P. D'Angelo[9], W. Dabrowski[10], P. Delpierre[11], A. Deneuville[12], W. Dulinski[7], B. van Eijk[13], A. Fallou[11], F. Fizzotti[14], F. Foulon[3], M. Friedl[1], K.K. Gan[15], E. Gheeraert[12], G. Hallewell[11], S. Han[15], F. Hartjes[13], J. Hrubec[1], D. Husson[7], H. Kagan[15,◊], D. Kania[15], J. Kaplon[16], R. Kass[15], T. Koeth[8], M. Krammer[1], A. Logiudice[14], R. Lu[14], L. mac Lynne[8], C. Manfredotti[14], D. Meier[16], M. Mishina[18], L. Moroni[9], A. Oh[17], L.S. Pan[15], M. Pernicka[1], A. Peitz[8], L. Perera[8], S. Pirollo[6], M. Procario[19], J.L. Riester[7], S. Roe[16], L. Rousseau[3], A. Rudge[16], J. Russ[19], S. Sala[9], M. Sampietro[4], S. Schnetzer[8], S. Sciortino[6], H. Stelzer[2], R. Stone[8], B. Suter[19], R.J. Tapper[20], R. Tesarek[8], W. Trischuk[21], D. Tromson[3], E. Vittone[14], A.M. Walsh[8], R. Wedenig[1], P. Weilhammer[16,◊], M. Wetstein[8], C. White[22], W. Zeuner[17], M. Zoeller[15]

[1] *Institut für Hochenergiephysik der Österr. Akademie d. Wissenschaften, Vienna, Austria*
[2] *GSI, Darmstadt, Germany*
[3] *LETI (CEA-Technologies Avancees) DEIN/SPE - CEA Saclay, Gif-Sur-Yvette, France*
[4] *Polytechnico Milano, Italy*
[5] *LENS, Florence, Italy*
[6] *University of Florence, Florence, Italy*
[7] *LEPSI, IN2P3/CNRS-ULP, Strasbourg, France*
[8] *Rutgers University, Piscataway, NJ, U.S.A.*
[9] *INFN, Milano, Italy*
[10] *Faculty of Physics and Nuclear Techniques, UMM, Cracow, Poland*
[11] *CPPM, Marseille, France*
[12] *LEPES, Grenoble, France*
[13] *NIKHEF, Amsterdam, Netherlands*
[14] *Univerity of Torino, Italy*
[15] *The Ohio State University, Columbus, OH, U.S.A.*
[16] *CERN, Geneva, Switzerland*
[17] *II.Inst. für Exp. Physik, Hamburg, Germany*
[18] *FNAL, Batavia, U.S.A.*
[19] *Carnegie-Mellon University, Pittsburgh, U.S.A.*
[20] *Bristol University, Bristol, U.K.*
[21] *University of Toronto, Toronto, ON, Canada*
[22] *Illinois Institute of Technology, Chicago, IL, U.S.A.*

◊ Spokespersons

Abstract

Over the past 18 months the RD42 collaboration continued the improvement of CVD diamond detectors for high luminosity experiments at the LHC. We have made extensive progress on the diamond quality, on the development of diamond trackers and on radiation hardness studies. Our original expectation was to complete the research and development phase by the end of 1999. However transforming the technology to the LHC specific requirements will take longer than anticipated. In this report we present the progress made and the requirements to complete the programme.

1 The RD42 1998/1999 Research Program and Milestones

During the past eighteen months the RD42 collaboration has continued to improve CVD diamond material for detector applications. We worked exclusively with one manufacturer and successfully transferred their basic growth recipe for detector-grade diamond from research reactors to production reactors. This allows the production of detector-grade material on large wafers. Fig. 1 shows a photograph of a free standing 10 cm diameter CVD diamond wafer to illustrate the appearance of the material. A large amount of high quality, production reactor diamond was produced and tested with dot and strip patterns. The best samples were selected for use as pixel devices. One outcome of this work is that we have planned a meeting at CERN on March 6, 2000 when the diamond manufacturer (De Beers [1]) will present their plans to the CERN community with regard to production and pricing.

Figure 1: Free-standing, 100 mm diameter CVD diamond (courtesy of De Beers Industrial Diamond Division (UK) Ltd.) [1].

Our work continued on the development of diamond pixel detectors. We obtained, tested and selected ten 1 cm × 1 cm high quality diamonds and turned then into pixel detectors. We have tuned our metallization techniques and have now demonstrated compatibility with most commercial bump-bonders. We recently produced diamond pixel devices with groups in ATLAS and CMS for evaluation. This work took longer to complete than we anticipated and thus these devices will be tested in the first half of 2000.

We have also successfully produced an SCTA 128 channel chip at TEMIC with an architecture compatible with the ATLAS tracker specifications. A diamond strip detector was tested with the SCTA 128 channel chip in a beam test at CERN. The beam test demonstrated excellent spatial resolution. A few minor complications in the chip design have been corrected and the chip will be re-submitted to TEMIC for a production run in a technology which is fully radiation hard.

Finally we have extended our radiation hardness studies of CVD diamond by irradiating diamond strip detectors with protons, and several diamonds with pions and neutrons. This year we will irradiate the highest quality production diamond which we recently received.

1.1 The LHCC Milestones

At the September 1998 LHCC meeting the RD42 renewal was approved with the following expectations [2]:

- RD42 should carry out their proposed further programme of work, with emphasis on pixel detectors and radiation hard electronics.

- RD42 should obtain price estimates and study production yields.

The RD42 referee's report also referred to the 1998 RD42/LHCC status report [3] which estimated that we would complete the RD42 programme by the end of 1999. As stated above the programme we outlined was quite ambitious and took longer than we estimated; we are still in the process of testing pixel devices and electronics, we have nearly completed the radiation hardness studies with the highest quality production diamond, and we are in the middle of a programme to produce even higher quality diamond.

1.2 Summary of Milestone Progress

During the last year we continued to receive high quality samples from the manufacturer. Our goal with these samples was to develop a set of parameters that would allow the transfer of the growth process from research reactors to production reactors. The manufacturer would not give us a price estimate or yield estimate until this process was complete. Eighteen months ago the collection distance of routine samples from the production reactor was approximately 120 μm with the best production diamonds having a collection distance of 150 μm. With twelve months of development the collection distance of routine production samples increased to 170 μm. Some of this production reactor diamond was irradiated and other pieces were tested as trackers in high energy pion beams at CERN. As of six months ago, the production reactor material, in general, was still lower in quality than that which is produced in the research reactor. However progress made during the last six months has now created production reactor diamond which is equal in quality to that produced in the research reactor. In addition we have discussed three avenues of research which may lead to higher quality diamond from the production reactors. These avenues will be pursued in the coming year.

RD42 has chosen a path to insure that the highest quality diamond is used to construct pixel detectors. This we felt is necessary given that bump-bonding and pixel electronics are in a state of rapid development. We have settled on a titanium/tungsten metallization for the pixel detectors. In addition, before a bump-bonder is given a high quality pixel detector they are asked to produce bumps on a practice diamond which has been prepared by the same method as the real devices. To date pixel devices were constructed for CMS and bump-bonded at UC Davis to the Honeywell version of the CMS/PSI chip. These devices are in the process of being tested at Fermilab and we hope to test them at CERN next year. In addition to the CMS pixel detectors we provided diamond pixel detectors for ATLAS to Bonn and Marseille. These devices will be bump-bonded in industry to the ATLAS FE-D pixel electronics. We are presently proceeding with the certification process. Once again we hope to test these devices at CERN in 2000.

Our program of testing the radiation hardness of CVD diamond has been extended to testing diamond strip detectors (previous tests used small diamonds with circular contacts) in proton and pion beams up to fluences of $4\times10^{15}/\mathrm{cm}^2$. In proton irradiations with one tracker we observed no loss of charge signal after $3\times10^{15}\ p/\mathrm{cm}^2$; after re-metallizating this diamond the observed charge signal increased. After exposing it to an additional $1\times10^{15}\ p/\mathrm{cm}^2$ we observed a 20 % loss in the charge signal indicating that a component of charge loss is contact damage rather than bulk damage. With a second tracker made from higher quality material we observed a 14 % loss of the mean charge after $1\times10^{15}\ p/\mathrm{cm}^2$. We also observed an improvement in the position resolution of all trackers which were irradiated. These results indicate that the production diamond has similar radiation hardness properties to that which is grown in the research reactor.

The remaining sections present details of the work outlined above.

2 Progress on the Improvement of CVD Diamond

Two important developments occurred in the improvement of detector grade CVD diamond during the past 18 months. While the first samples with 200 μm collection distances were developed during 1998, 1999 saw the consolidation of this quality of material where we received more than 20 samples of similar quality. Secondly, the technology to produce these samples was transferred to production reactors with a view to commercializing their production for future applications.

During the past year we have worked closely with De Beers to study the reproducibility of their diamond production process as well as to explore ways of improving the quality of the material. We have measured and characterized approximately twenty five 1×1 cm^2 samples from different growth runs and have fed our results back to them. Our results are consistent with only a few of these samples exhibiting collection distances of less than 150 μm. The pulse height distributions of two samples received in the last month is shown in Fig. 2. Two important and exciting characteristics illustrated in this figure are: the start of the charge distribution with more than 98 % of entries above 2000 e and the FWHM/MP of 1.0. These characteristics demonstrate the excellent quality of these diamonds.

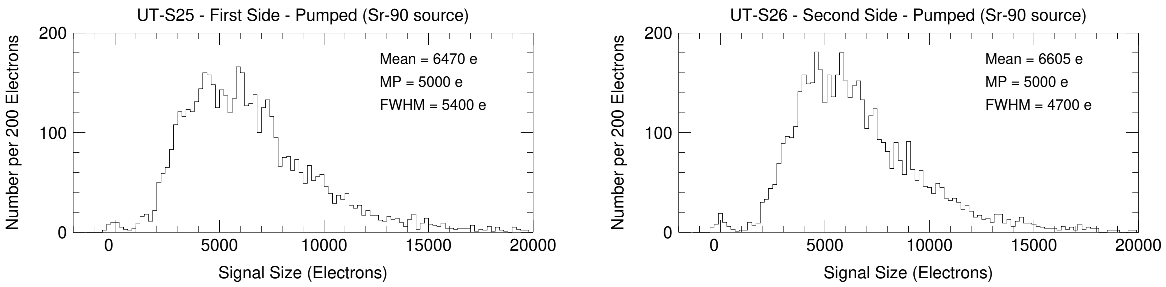

Figure 2: Pulse height distribution measured in two recent diamond samples using a ^{90}Sr β-source.

The large number of high quality samples received during the last 18 months has been crucial to feeding all of the detector studies RD42 has undertaken. This includes studies of the charge response uniformity and spatial resolution of high quality material to better understand what currently limits its quality with a view towards possible improvements.

Recently we received ten 2×4 cm^2 samples. Two of these have been patterned as strip trackers with 50 μm pitch and tested in beams. We are adapting our characterization stations to accept such large samples so that we can provide more rapid feedback on the quality of these samples with source characterisations. The manufacturer is now satisfied that they have developed a product with a collection distance between 150 μm and 200 μm and is prepared to market it for applications in particle physics. However, recent developments have indicated possible improvements to their process that could result in further increases in collection distance. To that end we have undertaken two new materials studies in collaboration with them.

One study involves quantifying the lateral uniformity of CVD diamond. Since the material is polycrystalline in nature the charge collection properties may vary from grain to grain. We have inscribed fiducial marks (laser cut in the surface) on three of the recently grown, high quality, CVD samples. One of these has undergone a series of tests by the manufacturer to localise the grain boundaries as well as to gain information about the internal structure of the poly-crystals. This sample has also been patterned into a strip tracker with 50 μm pitch and bonded to a VA2 readout chip [Fig. 3]. We recorded almost two million tracks with this tracker allowing us to measure the charge in 30×30 μm^2 cells with an average of 15 tracks. We observe regions of high mean signal and valleys of low mean signal. Crystals with lower pulse heights determine the low edge of the charge distribution and hence the maximum useful threshold that could be used in a diamond pixel detector. The study of this data is underway.

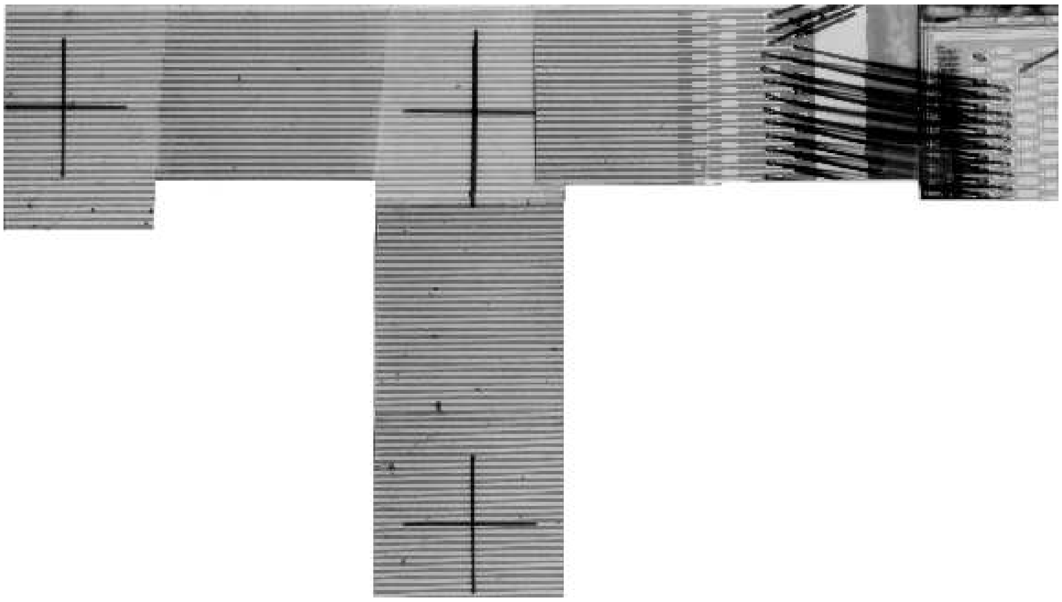

Figure 3: Photograph of the diamond strip detector CDS-59. The photo shows three laser cross marks on the surface of the diamond. The marks have been set for a precise alignment of uniformity maps obtained from beam tests and solid state studies on uniformity.

While the RD42 programme has undertaken over the last five years a number of studies of the properties of the highest quality CVD diamond material that has been developed, we are now in a position to move towards the development of full scale prototype diamond detectors for specific applications in high radiation regions of LHC (and other) experiments where its tolerance to dose should make it an alternative to silicon. To this end we have organised a meeting where prospective particle physicists, not necessarily those involved in the RD42 programme, can meet with diamond manufacturers to discuss the current state of the art in CVD material and the feasibility of using or developing material for particular applications in particle physics. This meeting will take place at CERN on March 6, 2000.

3 Results from Diamond Strip Detectors

During the last eighteen months RD42 tested diamond micro-strip detectors using the X5 pion beam at the SPS and the T9 beam at the PS. The main purpose of these tests was to characterize diamonds for their later use as pixel devices. The diamonds were characterized in terms of total charge collected and spatial resolution.

The position of tracks at the location of the diamond sensor was precisely determined using a silicon beam reference telescope. Fig. 4 shows a schematic drawing of the telescope.

Diamond sensors were mounted inside the reference telescope where the tracking precision is about 1 μm. This telescope was used in previous years. A thorough description can be found in references [3, 4, 5].

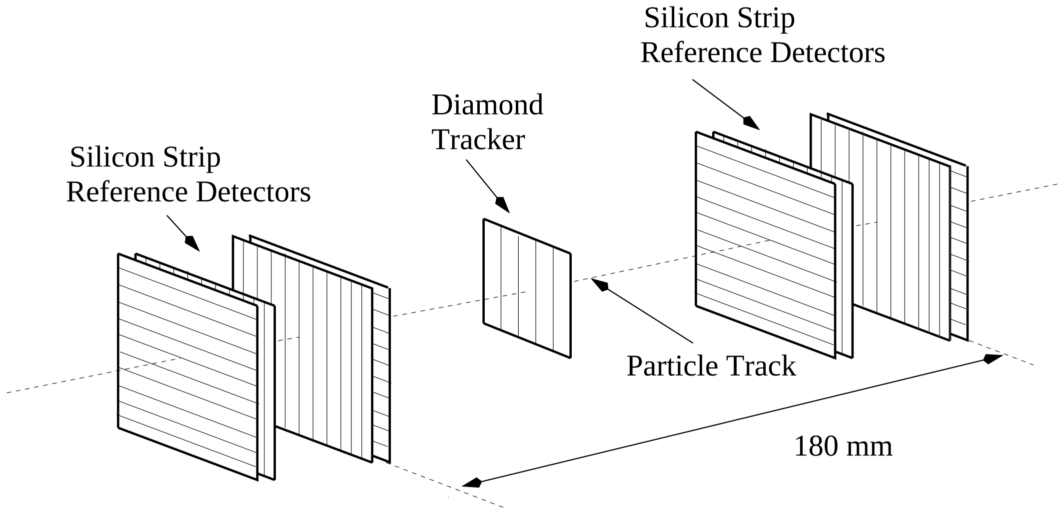

Figure 4: Schematic of the silicon beam reference telescope.

Fig. 5 shows a photograph of a 2×4 cm^2 CVD diamond strip detector. The strips on the growth side of the diamond were 25 μm wide on a 50 μm pitch. A solid electrode was on the nucleation side where a voltage of typically 500 V was applied. In total 256 strips of the detector were read out by two low noise CMOS chips (VA2 [6]).

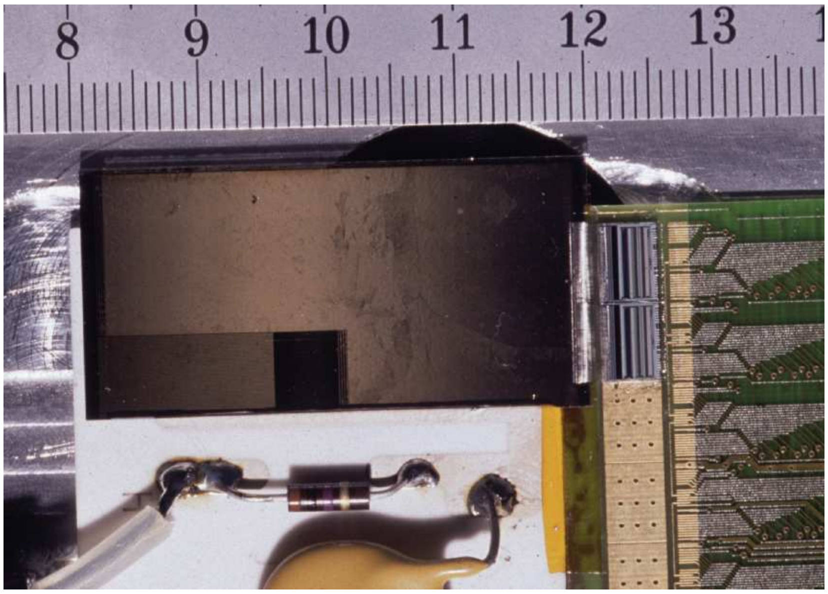

Figure 5: Photograph of a 2×4 cm^2 CVD diamond strip detector. The strips on the diamond surface were 25 μm wide on a 50 μm pitch. In total 256 strips of the detector were read out by two low noise CMOS chips (VA2).

3.1 Beam Test Results from a Diamond Sensor

We define the response of a detector plane to a particle which intersects that plane a *hit*. In a *cluster analysis* this hit is found by searching for a strip with the highest charge signal which exceeds a signal-to-noise threshold. A hit cluster includes neighbouring strips with charge signals above a lower signal-to-noise threshold. The sum of charge signals in the hit cluster gives the hit cluster charge. Fig. 6 shows the distribution of 2-strip cluster charge signals in diamond sensor CDS-69, and from a silicon strip sensor of the telescope. The cluster charge is presented in units of the single strip *rms* noise charge. The single strip *rms* noise charge is ≈ 100 e (strip length 6.4 mm) in diamond and ≈ 200 e in silicon (strip length 12.8 mm). In the diamond sensor the mean value signal-to-noise is 72-to-1, the most probable signal-to-noise is 50-to-1.

In a *transparent analysis* the pulse heights of the strips closest to the track are used independent of any threshold. The sum of charge signals closest to the track gives the transparent charge signal. Fig. 7 shows the distribution of transparent charge signals in units of the single strip noise. Four distributions are shown corresponding to the transparent charge signal from one, two, three and four strips. The distributions shift towards higher signal as more strips are included in the sum. The mean 2-strip transparent charge signal-to-noise is 58-to-1. The most probable 2-strip transparent signal-to-noise is about 40-to-1.

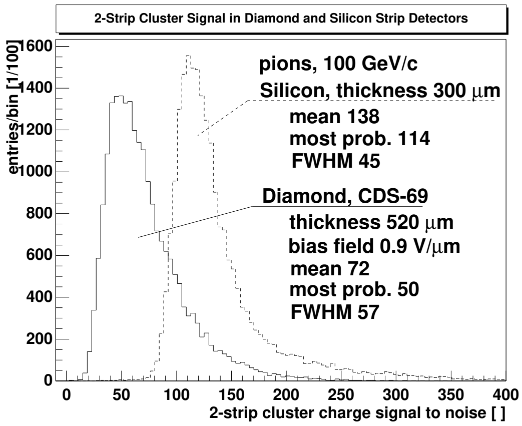

Figure 6: Distribution of charge signals from two strips in diamond (solid line) and in silicon (dashed line). The charge signal is normalized to the *rms* noise charge measured on single strips in diamond and in silicon respectively.

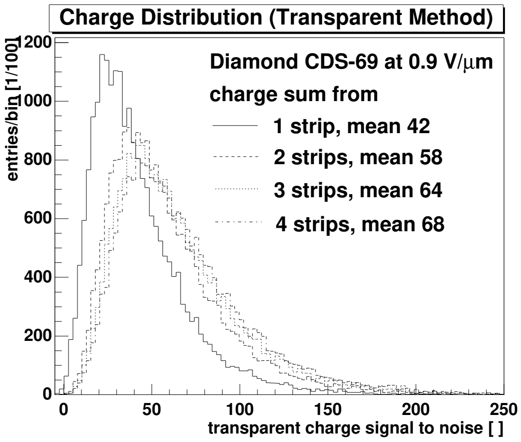

Figure 7: Distributions of the charge signals from strips nearest to the particle track. Four graphs are shown corresponding to the distribution of charges from one, two, three and four strips nearest to the track. The charge signals are normalized to the single strip noise charge.

The transparent analysis allows one to measure the charge collected on a single strip as a function of the track position relative to the strip. Fig. 8 shows two dimensional histograms of the charge signal from a single strip in diamond (left) and in silicon (right). One dimension (vertical) gives the charge signal in units of the single strip noise, the other dimension (horizontal) gives the position relative to the center of the strip which is taken to be zero (the principal strip). The entries of the histogram are grey scale coded. A profile plot is superimposed (cross marks) that gives the mean charge signal in units of the noise as a function of the track position. In the diamond the central strip occupies the region from -12.5 μm to +12.5 μm, while the adjacent strips occupy the region from -37.5 μm to -50 μm and +37.5 μm to +50 μm. This figure illustrates that the charge signal is almost independent (flat top) of the position of the track when the track passes through the strip where the charge signal to noise is 49-to-1. In between the strips a linear relation is observed indicating charge sharing between strips. It can be seen that the charge on adjacent neighbouring strips is around 8-to-1 which is 15 % of the level at the flat top region. The same method was used to investigate the behaviour in silicon (right histogram). The central strip in silicon is much narrower than in diamond and has a flat top with a level of 130-to-1. The adjacent readout strips are at -50 μm and +50 μm. There are two intermediate strips in between of two readout strips. As with diamond the charge signal is almost independent of the position of the track when the track passes through the strip. In silicon the mean charge on adjacent strips is around 5 corresponding to 4 % of the level at the flat top.

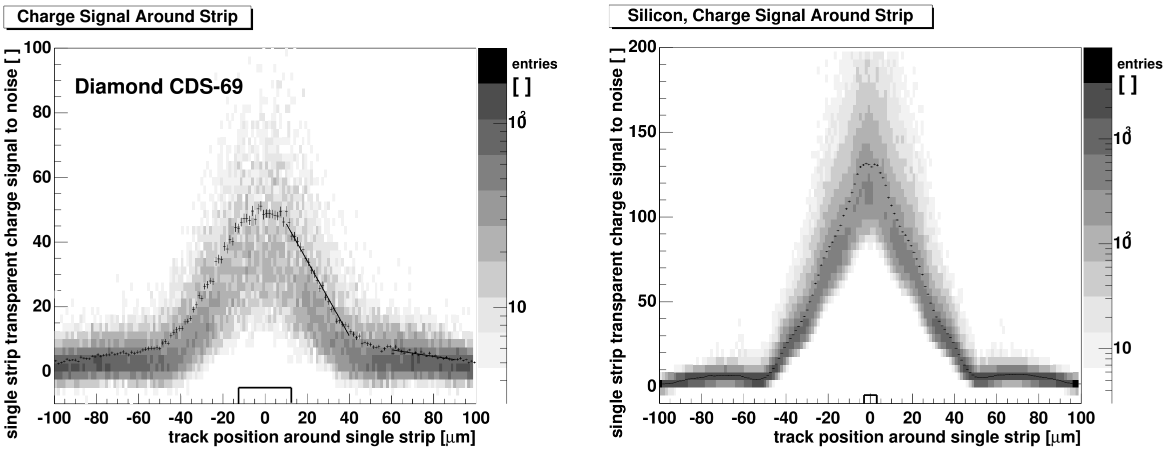

Figure 8: Charge signal from single strips in diamond (left) and in silicon (right) as a function of the position of the track. The charge signal is normalized to the *rms* single strip noise charge. The histogram represents the charge distribution where the number of entries are gray scale coded; the cross marks are the mean values of the distributions parallel to the ordinate.

Fig. 9 shows two dimensional histograms of the charge signal from two strips in diamond (left) and in silicon (right). Again, one dimension (vertical) gives the charge signal in units of the single strip noise, the other dimension (horizontal) gives the position relative to the strips. In diamond the graph of the averages (cross markers) are trapezoidal with a flat top. The flat top extends from the left edge of the left strip to the right edge of the right strip. There is nearly no charge loss between the strips. The charge signal level of the flat top is 58 (in agreement with the 2-strip mean charge from Fig. 7). One can see that the charge from two strips is higher than the charge from a single strip at its flat top. Two strips collect more charge since there is always charge induced on adjacent strips even if the track passes through the principal strip. In silicon the graph of the mean values peaks at the position of the readout strips. In the region between strips there is charge lost due to the capacitive coupling of the strips to the intermediate strips and from there to the backplane.

The hit position is determined from the charge signal on strips. In particular the charge on the seed strip and the next highest charge on the adjacent strip can be used (two strip center of gravity method) to derive the position of the hit

$$u_{\mathrm{h}} = u_{\mathrm{l}} + \eta_{\mathrm{r}} \cdot P \tag{1}$$

where u_{l} is the position of the left strip, P is the strip pitch and $\eta_{\mathrm{r}} = q_{\mathrm{r}}/(q_{\mathrm{r}} + q_{\mathrm{l}})$ is the fractional charge on the right strip. There are other methods of determining the hit position: the digital method uses the position of the principal strip, the K-strip method uses the center

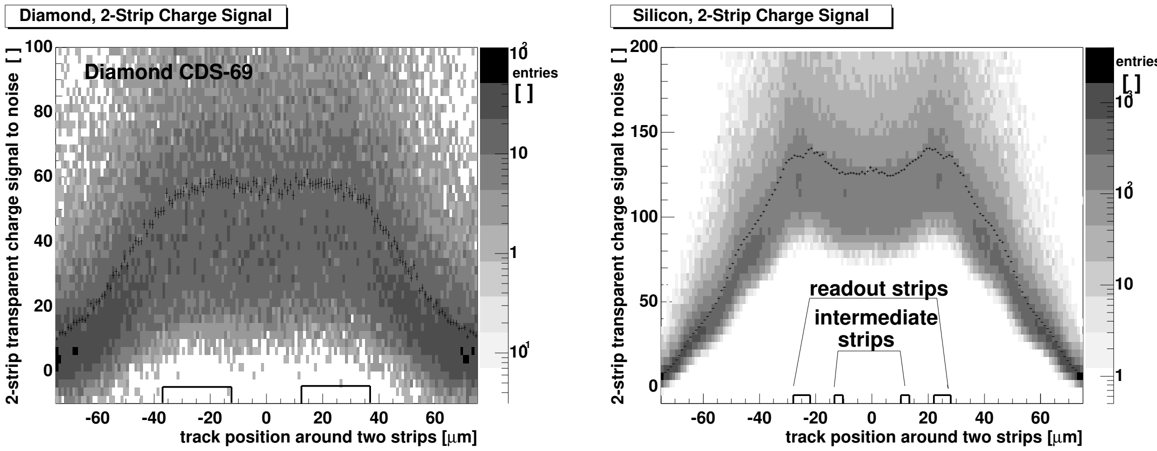

Figure 9: Charge signal from two strips in diamond (left) and silicon (right) as a function of the position of the track. The charge signal is normalized to the *rms* single strip noise charge. The histogram represents the charge distribution where the number of entries are gray scale coded; the cross marks are the averages of the distributions parallel to the ordinate.

of gravity of the charge on K adjacent strips. Fig. 10 shows distributions of residuals using three different methods. The upper measurement was obtained using a diamond tracker with 10 μm wide strips on a 50 μm pitch. The lower measurement was obtained using a diamond tracker with 40 μm wide strips on a 50 μm pitch. It can be seen that the width of the distribution depends on the method chosen. Using the two strip center of gravity method the spatial resolution is smaller than using either the digital method or the K-strip center of gravity method and smaller than the theoretical digital resolution of $50/\sqrt{12}$ μm $= 14.4$ μm.

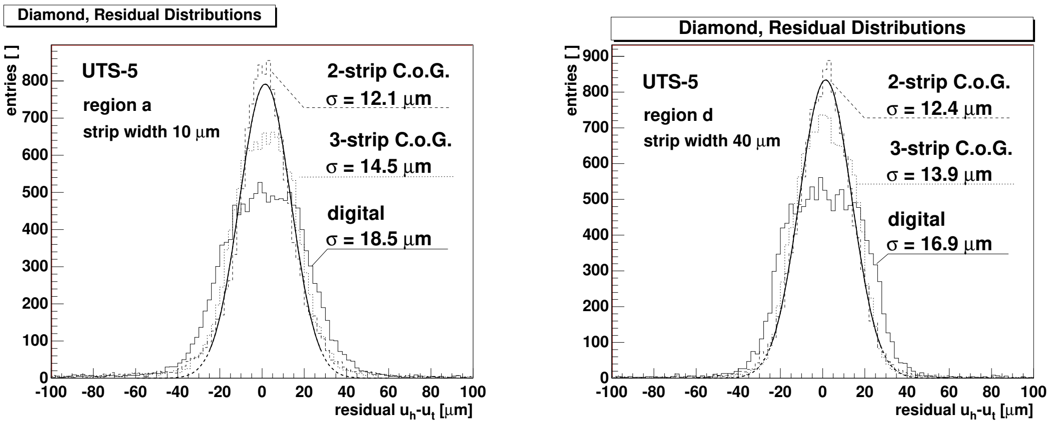

Figure 10: Residual distributions of the diamond detector with 10 μm wide strips in region a (left) and 40 μm wide strips in region d (right). The distributions for the 2-strip center of gravity, the 3-strip center of gravity and the digital hit finding methods are shown.

3.2 Uniformity Studies

CVD diamond is inherently polycrystalline in nature whereas silicon is mono-crystalline. This morphological difference may influence the charge collection properties laterally across the sensor. Pictures of mean charge collected laterally across the sensor can be taken by illumination in particle beams. Regions of high mean signal and valleys of low mean signal were observed in CVD diamond detectors using this method. The level of signal uniformity in a CVD diamond sensor and a silicon sensor were studied. In CVD diamond the level of uniformity changes with length scale. The signal charge distribution from macroscopic regions of several millimeters were found to be a convolution of signal distributions with high and low signal charge from microscopic regions.

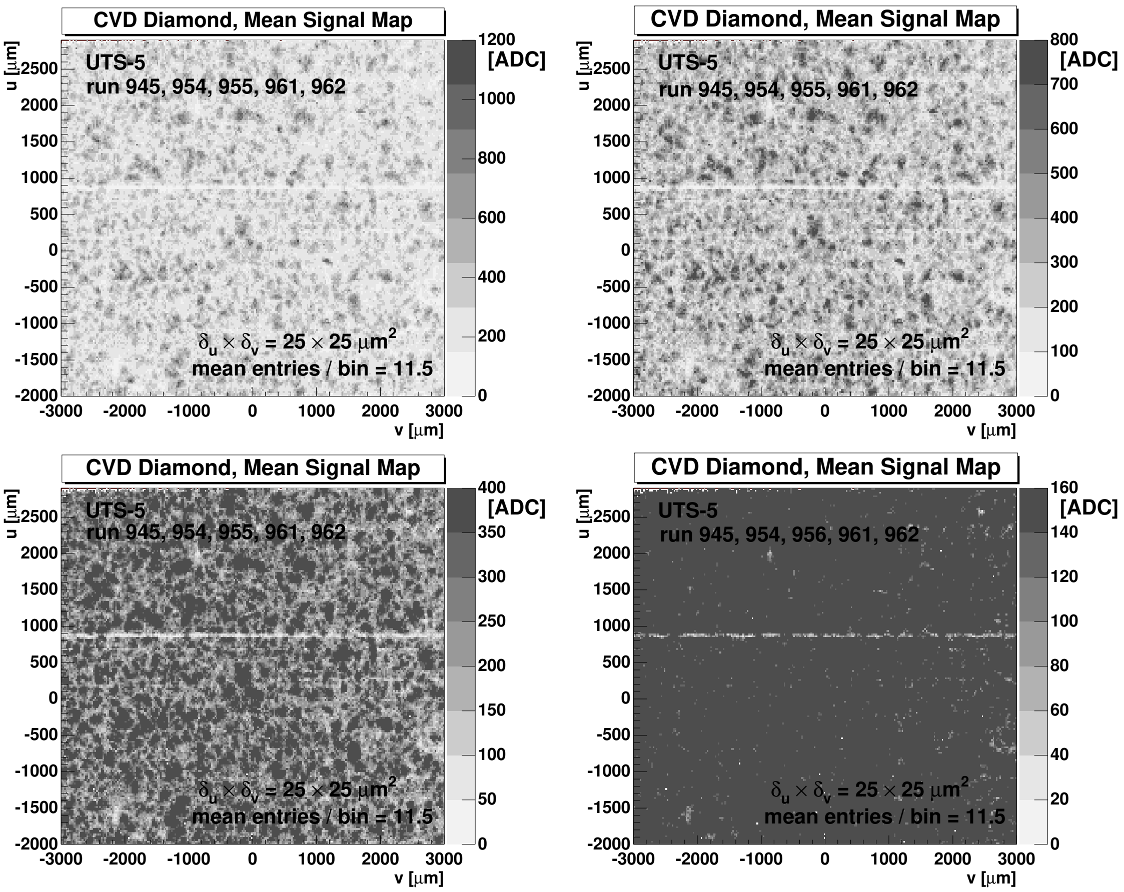

Figure 11: Mean collected charge in diamond detector UTS-5 as a function of the position of the particle track. The mean charge is gray scale coded and measured in bins of 25 μm $\times$ 25 μm. Four maps are shown. The maps are based on the same data. The maps differ in the ADC range chosen.

Fig. 11 shows the mean signal map of the diamond detector UTS-5 on a bin scale of $\delta_u \times \delta_v = 25\ \mu\text{m} \times 25\ \mu\text{m}$. Each bin contains on average 11.5 entries. In the upper maps one observes regions of higher and lower mean signal. It can be seen that the mean signal fluctuates from bin to bin. It can also be seen that there are contiguous regions where the bins have the same gray-scale-code. There are dark regions (spots) and light regions. The lower maps were prepared in order to emphasize regions with mean signals at the lower end of the charge distribution (around the most probable signal and below the most probable signal charge). The map with $Q_{\max} = 160$ ADC shows very few ($\approx$15) bins which have a mean signal below 20 ADC.

Fig. 12 shows a histogram of the normalized mean values from signal maps of a silicon and a CVD diamond strip detector. The mean values were measured using a bin size of 100 μm$\times$100 μm. The mean value of each distribution is normalized to the *average mean over all bins*, $\bar{Q} = \frac{1}{B}\sum_{b=1}^{B} \bar{Q}_b$. The measured distribution is a convolution of two distributions:

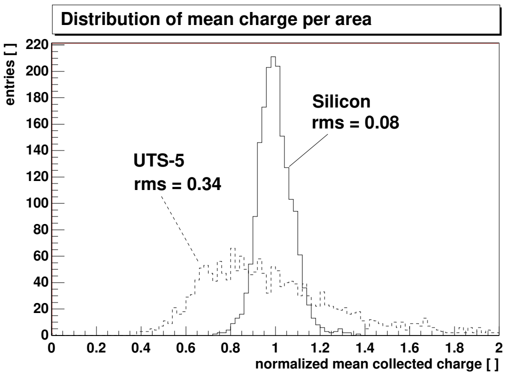

Figure 12: Distribution of mean charge signal in silicon and diamond (UTS-5) taken from a signal map with bin size of 100 μm $\times$ 100 μm and about 46 events per bin.

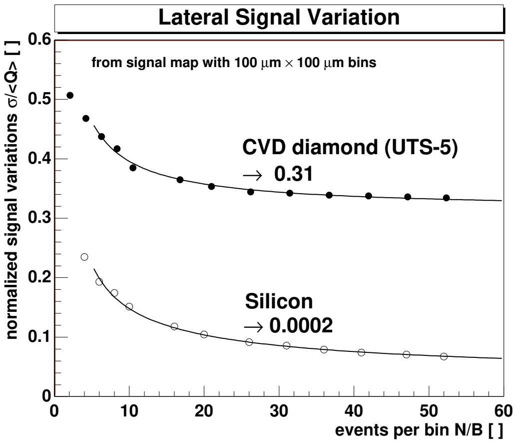

Figure 13: Normalized variation, $\hat{\sigma}_{\mathrm{m}}$, of mean signals from silicon and diamond (UTS-5) as a function of the mean number of entries in bins. The bin size is 100 μm$\times$100 μm. The points are measurements, the solid line is a fit from the model [Eq. 2].

firstly statistical variations of the inherent Landau fluctuations and the noise fluctuations which have the variance $\mathrm{VAR}(Q_b)$. Secondly there is a systematic variation from bin to bin whose distribution is unknown. The systematic variation of the mean signal has the variance $\mathrm{VAR}(\bar{Q}_b)$. The normalized mean signal variation, $\hat{\sigma}_{\mathrm{m}}$, measured from the histogram *rms* of Fig. 12 is then expressed in terms of the statistical variation and the bin-to-bin variation:

$$\hat{\sigma}^2_{\mathrm{m}} = \frac{1}{\bar{n}} \cdot \frac{\mathrm{VAR}(Q_b)}{\bar{Q}^2} + \frac{\mathrm{VAR}(\bar{Q}_b)}{\bar{Q}^2}. \tag{2}$$

The term containing statistical variations decreases asymptotically as $1/\bar{n}$. The systematic variation does not decrease as $1/\bar{n}$ and is independent of the number of entries per bin.

A measurement of the normalized variation as a function of the mean number of entries per bin is shown in Fig. 13. The variation in diamond and silicon decrease as expected asymptotically with increasing number of entries per bin. At entries $\bar{n} \geq 5$ the measured variation is well approximated by Eq. 2 which is shown as a fit to the data. At the given scale of 100 μm $\times$ 100 μm the value for infinite number of entries per bin is 0.31 in diamond and close to zero in silicon. The value for infinite number of entries was found from the fit to the data. We associate in the fit the asymptotic value with the systematic variation. The systematic variation allows one to define the *signal uniformity of the detector*

$$\mu \stackrel{\mathrm{def}}{=} 1 - \frac{1}{\bar{Q}} \cdot \sqrt{\mathrm{VAR}(\bar{Q}_b)} \stackrel{\mathrm{Eq.\ 2}}{=} \lim_{\bar{n}\to\infty} (1 - \hat{\sigma}_{\mathrm{m}}). \tag{3}$$

where μ takes values between 0 to 1 or 0 % to 100 %. On the chosen scale of 100 μm$\times$100 μm the uniformity of silicon is close to 100 % and the uniformity of the diamond UTS-5 is ≈69 %.

In the coming year, there are open issues which will be studied in conjunction with the diamond manufacturer. Firstly the mean residual of tracks as a function of the position. Secondly the spatial resolution as a function of the position. And the width of the signal distribution as a function of the position. The outcome of these tests may yield information about material properties which will help improving the diamonds.

3.3 Diamond Strip Detectors with fast Analogue SCT Readout

In our last reports [3, 7] we showed results from diamond strip detectors using the 32 channel version of the analogue SCT/DMILL front end operating at 40 MHz. Our goal is to demonstrate a detector/electronics combination which yields 10-to-1 most probable signal-to-noise at 25 ns signal peaking time. A follow-up version of the SCT32A chip was designed in 1997 and was submitted to TEMIC (DMILL) in November 97 sharing an engineering run with the ATLAS SCT and LHC-B RICH projects. The design aimed at optimisation of performance for the relatively low input capacitance of diamond detectors. The chip now has 128 channels, a pipeline with 128 cells, an input stage in each channel optimised for diamond strip detectors and a control block including power supply DACs and control and monitoring functions. The data protocol follows ATLAS specifications. Each channel of this chip consists of a bipolar preamplifier shaper input stage followed by a 128 cell analogue pipeline and a 128-channel output multiplexer operating at 40 MHz. The shaper provides a signal with a peaking time of 21 ns to 25 ns depending on the capacitive load. The analogue pipeline samples the output of the shaper at 40 MHz clock frequency. The chip was produced in radiation hard DMILL technology which is radiation hard up to 10 Mrad corresponding to a fluence of 3×10^{14} particles/cm^2. At the time when this chip was processed the technology was still evolving. In particular resistors were not radiation hard and details of the bipolar process were still to be modified. The technology was officially released with radiation hardness guaranteed up to 10 Mrad in November 1998.

The chip was delivered in the middle of 1998. Full functionality of the chip has been demonstrated. Measurements show a noise performance of ENC$\approx$ 620 e [8]. Fig. 14 shows the mean single pad charge measured in a silicon pad sensor in the pion beam. The mean charge was sampled as a function of the time between the pipeline clock phase and the event trigger. The measurement is shown for the time interval from 0 ns to 75 ns corresponding to 3 cells of the analogue delay buffer (ADB). It can be seen that the mean signal peaks at about 25 ns. The measurement illustrates the semi-Gaussian (CR-RC^3) shape of the signal as it is produced at the output of the shaping amplifier.

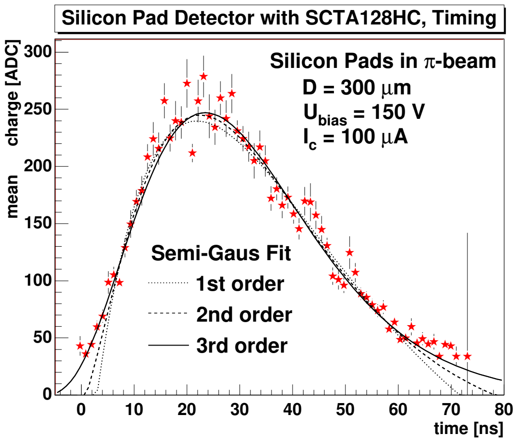

Figure 14: Mean signal from single pads in the silicon pad detector with SCT128HC readout as a function of the time between trigger and pipeline clock phase. The measurement is fitted with the semi-Gaussian function for the orders $n = 1$, $n = 2$ and $n = 3$.

The SCT128HC chip was used to read out a diamond sensor (UTS-5) in a testbeam. The diamond was bonded to exactly the same SCTA128HC readout chip which was used for the measurement with the silicon pad detector. The chip was operated at the same pre-amplifier current as for silicon and the gain on UTS-5 is assumed to be equal to the gain in the silicon pad detector. Fig. 15 shows the 3-strip transparent signal as a function of time between pipeline clock phase and the trigger. The same semi-Gaussian shape is observed as on the silicon pad-detector The signal peaking time of 25 ns can be read from this figure. Using a timing window from 40 ns to 50 ns one obtains the signal distribution from the transparent analysis shown in Fig. 16. With a single strip noise of 5.0 ADC the mean and most probable signal-to-noise ratios are 10-to-1 and 7.2-to-1. Using the gain measurement from silicon pad sensors one obtains a mean signal of 6000 e in diamond UTS-5.

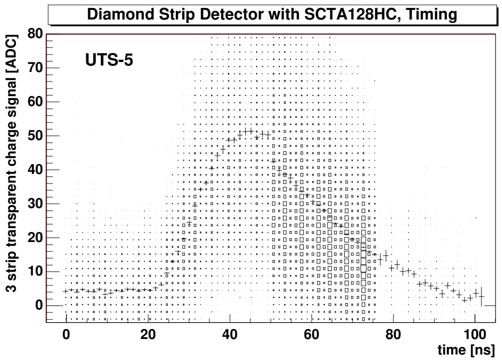

Figure 15: Transparent signal from 3 strips of the diamond detector UTS-5 with SCTA128HC readout as a function of the TDC time between trigger and pipeline clock phase. The mean values at each time bin are superimposed with crosses.

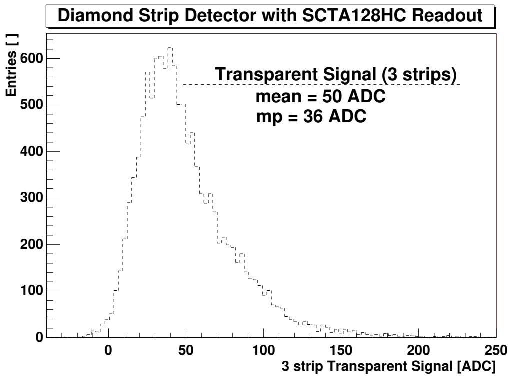

Figure 16: Charge signal distribution from the diamond strip detector (UTS-5) with DMILL/SCTA128HC readout electronics. The charge signals are the sum from 3 strips nearest to the track (transparent analysis).

Fig. 17 shows the distribution of the residuals using the K-strip center of gravity method (K is the number of strips included in the hit cluster). The distribution peaks at 0 μm and the Gaussian fit gives the spatial resolution of 16.5 μm. Based on the results from trackers with VA2 readout we expect an improvement in spatial resolution using the 2-strip center of gravity method.

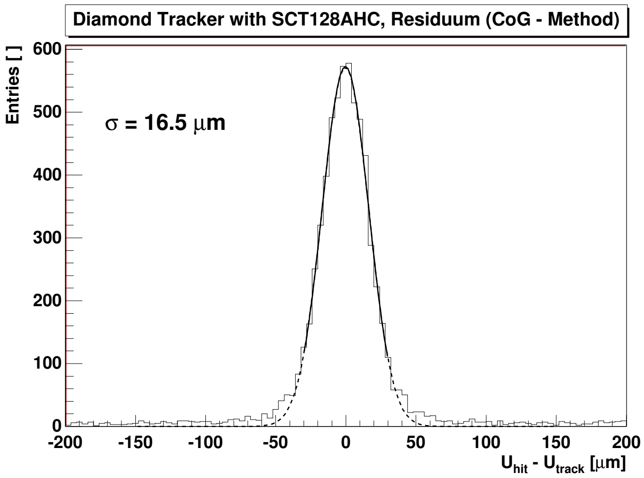

Figure 17: Residual distribution from the diamond strip detector UTS-5 with DMILL/SCTA128HC readout electronics. The K-strip center of gravity method was used for hit finding. The measured residual distribution is fitted by a Gaussian function (solid line) with a standard deviation of $\sigma = 16.5$ μm.

The DMILL technology is now tested to be radiation hard up to 3×10^{14} p/cm^2 and 10 Mrad. The irradiation tests were carried out with the binary chips ABCD, which is the baseline option for the ATLAS SCT [9]. Taking into account some shortcomings in the present 128 channel SCTA chips which were detected while analyzing the data taken with silicon detectors connected to the SCTA chip, improvements have been implemented in a new version of this chip. The re-design work finished in December 1999 and the new chip will be submitted in January 2000. The front end of the new chip is nearly identical to the front end part of the ABCD chip. The noise for the ABCD has been measured to be 420 e ENC without external load before irradiation and 580 e ENC after exposing it to 3×10^{14} p/cm^2. The new SCT128HC chip will be mounted on 2×4 cm^2 diamond trackers and studied in a beam test in summer 2000.

4 Irradiation Studies of CVD Diamond Sensors

The ability of the innermost tracking detector material to continue to function after exposure to large radiation dose and high particle fluxes is crucial for the success of the LHC. The consequences of high radiation dose in silicon are well known: large increases in leakage current and smaller observed charge. As a result the signal-to-noise ratio in damaged detectors decreases rapidly.

A significant part of the RD42 programme is to continually test the newest material for its radiation hardness properties. In the last status report [3] we presented evidence that diamonds produced in research reactors had no observable increase in leakage current up to fluences of 2×10^{15}/cm^2 independent of whether the particles were protons, neutrons or pions. It was also shown that the charge signal decreases at high fluences depending on the particle type. After irradiation entries in the tail of the signal distribution appear closer to the most probable signal. It was shown that for diamonds with charge collection distances up to 100 μm the most probable charge is reduced by 20 % at approximately 5×10^{15} protons/cm^2 and 1.5×10^{15} pions/cm^2.

Irradiations with protons, pions and neutrons have been carried out in the last eighteen months (1998 and 1999) with higher quality diamonds with collection distance around 150 μm and with diamond strip detectors. There are first results on the effect of radiation on spatial resolution in addition to charge collected.

4.1 Proton Irradiation

In June 1997 and Oct./Nov. 1999 the latest diamond samples at that time and diamond trackers previously tested were irradiated at the Proton Synchrotron (PS) at CERN. The protons had a momentum of 24.3 GeV/c. The average proton flux was 4×10^{10} p/cm^2/s. The absolute proton fluence was measured using aluminium foils. Fig. 18 shows the pulse height distribution of one of the samples irradiated in 1999 before and after irradiation with 1×10^{15} p/cm^2. This diamond shows a reduction in the most probable charge of 15 % at this fluence. The low end of the pulse height distribution changes very little.

Fig. 19 shows the signal to noise distribution from a diamond tracker before and after 1×10^{15} p/cm^2. At this fluence the most probable signal (or signal to noise ratio) is decreased by 15 % consistent with the data measured on the sample shown in Fig. 18. Fig. 20 shows the residual distribution before and after 1×10^{15} p/cm^2. It can be seen that the spatial resolution improves by 18 % after irradiation. This effect is statistically significant since the device is physically the same before and after irradiation and the same tracking program was used to analyze each data set.

Fig. 21 shows the normalized spatial resolution versus fluence. In this plot the before irradiation resolutions varied from 10 μm to 15 μm. In all cases the after irradiation spatial

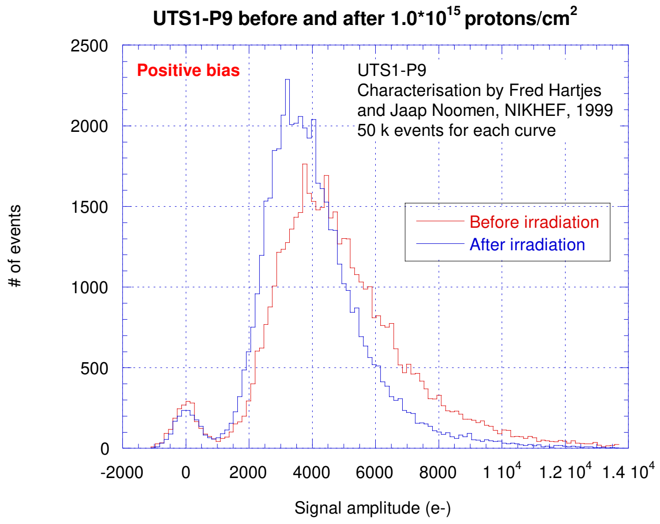

Figure 18: Distribution of the induced charge signal by ^{90}Sr in diamond UTS-1-P9 before and after proton irradiation.

resolution is better than the before irradiation resolution. The cause of this effect is presently being studied.

Fig. 21 together with the pulse height distributions demonstrates an additional effect previously observed in diamonds irradiated with a solid circular pattern. The two data points at a fluence of 3×10^{15} p/cm^2 come from the same diamond before (higher point) and after (lower point) remetallizing the diamond with a new metal. The spatial resolutions observed at this fluence are statistically consistent indicating that the re-metallized tracker is performing properly. However it was observed that the charge in the re-metallized tracker was 22 % larger than before re-metallization. Thus we see no change in spatial resolution but a significant change in signal size. This suggests that a substantial fraction (≈ 22 %) of the "apparent" damage was due to poor contact and not bulk diamond damage. Since the contacts used in these tests were Cr/Au (which is not proposed for the LHC), a thorough test of the Ti/W contacts used in pixel detectors will be performed in the year 2000.

4.2 Pion Irradiation

In 1999 the pion irradiation program of testing the latest available CVD diamond samples was continued at PSI/Villigen. As before the pions (π^+) had a momentum of 300 MeV/c. Until 1998 we irradiated diamond samples with charge collection distance in the range from 50 μm to 130 μm and results were shown in the previous report [3]. In 1999 we irradiated samples with initially ≈ 180 μm charge collection distance.

Fig. 22 shows the mean signal (left) and the most probable signal (right) normalized to the unirradiated signal as a function of pion fluence. The most probable signal decreases by 40 % at at 1×10^{15} π/cm^2. The analysis of the signal distributions (not shown) demonstrates that the lower edge of signal distributions does not change with fluence. The new data presented here is preliminary and further studies will be undertaken as soon as their radio-activity allows transportation and handling. One study is the effect of the contacts on the collected charge.

Two diamond trackers were irradiated at PSI in Sept. 1999. These devices were to "hot" to allow transport to CERN for our last beam test in November 1999. We are requesting beam time to test these device in the year 2000.

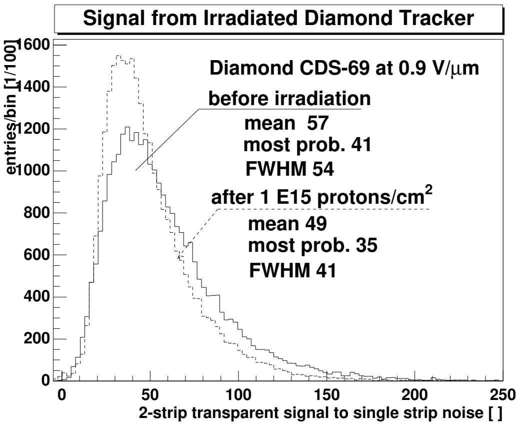

Figure 19: Charge signal distribution from two diamond strip detectors before and after irradiation with 1×10^{15} p/cm^2. The signal is the sum of charges from two strips nearest to the track (transparent method). The signals are normalized to the single strip noise charge.

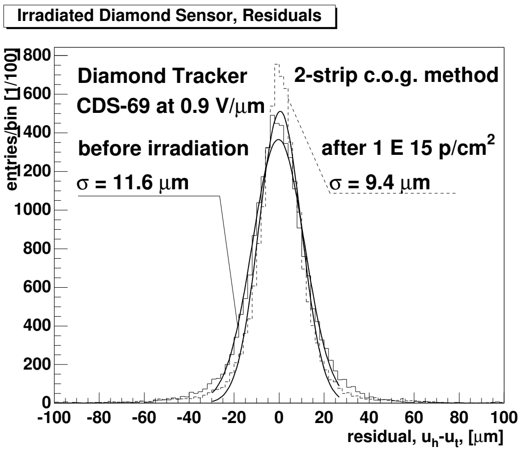

Figure 20: Distribution of residuals, $u_\mathrm{h} - u_\mathrm{t}$, before (solid line) and after (dashed line) irradiation with 1×10^{15} p/cm^2. The distributions are fitted by Gaussian functions, centered at zero, with a standard deviation, σ, which gives the spatial resolution of the diamond strip detector.

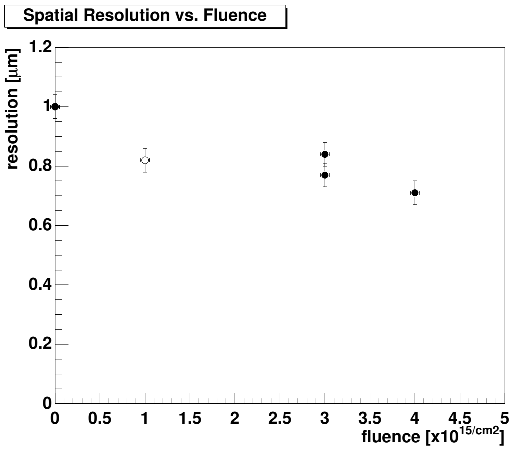

Figure 21: Spatial resolution in diamond trackers, normalized to the before irradiation resolution, as a function of particle fluence.

4.3 Neutron Irradiation

From 1995 to 1997 diamond samples were irradiated with neutrons at ISIS at RAL [5]. The neutrons at ISIS had an energy spectrum that peaks at 1 MeV. Fig. 23 shows the normalized charge collection distance as a function of the neutron fluence. The diamonds used for these irradiations initially had a charge collection distance of 40 μm to 50 μm. This data suggests no change in charge collection distance up to 0.4×10^{15} n/cm^2. The charge collection distance has a transition between 0.4×10^{15} n/cm^2 and 0.5×10^{15} n/cm^2 and decreases towards higher neutron fluences.

In 1998 and 1999 new diamond samples with initially 120 μm charge collection distance were irradiated at ATOMKI in Debrecen and Saclay. The neutron energy spectrum at ATOMKI differs from ISIS: at ATOMKI the spectrum begins at 0.4 MeV and is almost flat up to 17 MeV where it cuts off. Fig. 24 shows the normalized mean signal as a function of the neutron fluence from the Debrecen data. At a fluence of 0.9×10^{15} n/cm^2 the normalized mean signal is decreased by 25 %. In comparison with the ISIS data, the ATOMKI data shows a smaller decrease towards higher fluence. The effects of contacts and the difference

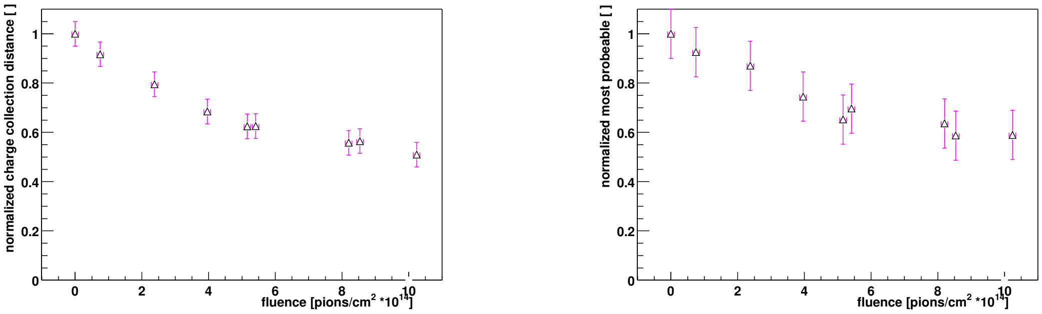

Figure 22: PSI/Villigen pion irradiation 1999: normalized mean signal (left) and normalized most probable signal (right) as a function of the pion fluence. The initial charge collection distance on these samples was about 180 μm.

in the two irradiations are being studied.

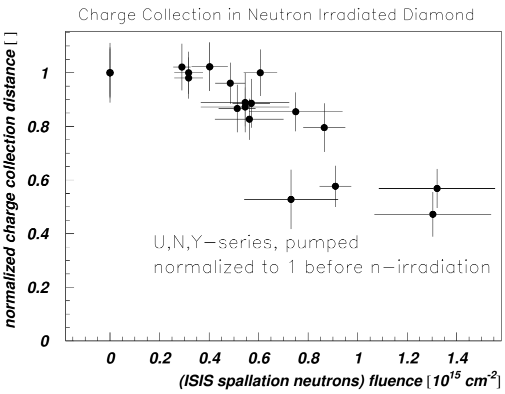

Figure 23: ISIS/RAL neutron irradiations on $ccd \approx 50$ μm diamonds: normalized charge collection distance as a function of neutron fluence.

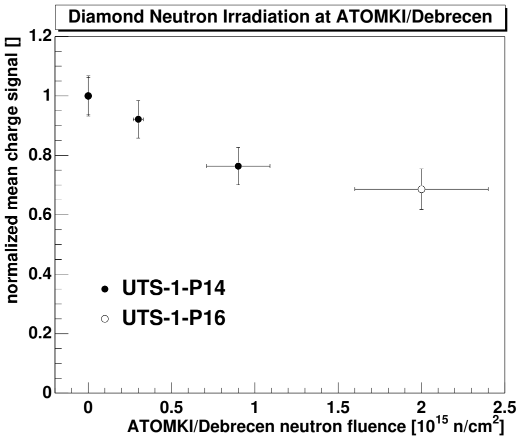

Figure 24: ATOMKI/Debrecen neutron irradiations on $ccd \approx 120$ μm diamonds: normalized charge collection distance as a function of neutron fluence.

5 Diamond Pixel Detectors

Pixel detectors cover the central region of the beam pipe in both the ATLAS and CMS detectors. Devices in this region will have to withstand very large doses of particles. The results of the previous sections show that diamond is a viable detector material and has the required radiation tolerance. However applicability for use in the LHC requires a demonstration of a working pixel detector together with working electronics. Since the RD42 collaboration has not developed pixel electronics it collaborates with members of several LHC experiments in order to demonstrate the applicability of diamond pixel devices for those experiments. During the past few years we have begun such collaborations. The successes of these collaborations have been mixed due to the general difficulty of bump-bonding small devices (*e.g.* 1 cm $\times$ 1 cm) to electronics. This past year we have worked with bump-bonders and finalized a metallization process that appears to be compatible with industrial bump bonding technology and can be used on small parts. Ten diamond pixel devices have been fabricated and are presently being bump-bonded. We plan to test these devices in particle beams in the coming year.

5.1 Diamond Pixel Sensors for CMS

Fig. 25 shows a picture of the upper right corner area of a pixel detector prepared for the CMS experiment after bumps were deposited. The pixels were 100 μm squares and the pixel pitch for this version of the CMS electronics was 125 μm in both directions. The pattern on the diamond was 24 pixels $\times$ 36 pixels; the electronics pattern was 22 pixels $\times$ 32 pixels. Fig. 25 shows the diamond pixels at the edge, the clarity of the pixel pattern lithography and the cleanliness of the bump production. The metallization on the diamond was Ti/W. The bump metal was indium and the bump efficiency was measured to be 100 %. This is a large improvement over the 30 % efficiency achieved with CMS devices last year [3]. Fig. 26 shows an enlargement of a single bump focused on the top of the bump (left) where the pad is out of focus and focused on the pad (right) where the bump surface is out of focus. The bumps are approximately 10 μm high. These photographs are typical of the bumps on this device. The bump metal adhesion was measured using the practice part and was well above the minimum requirement for good electrical connections.

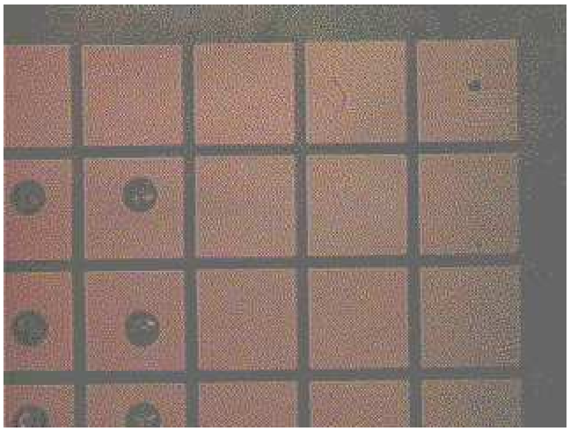

Figure 25: Photograph of the upper right corner area of a pixel detector prepared for CMS after bumps have been deposited.

Two diamond pixel detectors were bump-bonded to the radiation hard Honeywell version of the CMS pixel electronics. These devices were mounted and wirebonded on hybrids. They are presently being tested at Fermilab in a pion beam. We expect preliminary results in early January and propose to continue these tests at CERN after the Fermilab testbeam ends in late January 2000.

5.2 Diamond Pixel Sensors for ATLAS

Fig. 27 shows a picture of the edge of a diamond pixel detector prepared with the ATLAS pixel pattern. The pixels are 25 μm wide by 375 μm long. Both solder and indium bump-bonding is planned for these devices. For solder bonding a Cr/Au layer will be added to the Ti/W pixel pattern at the position of the solder bumps. SOFRADIR working together with LETI will add the Cr/Au layer, the solder bumps and perform the flip-chiping. To handle the 1 cm $\times$ 1 cm diamond a silicon wafer has been prepared in which the diamond is embedded. This work is presently underway. The electronics used will be the ATLAS FE-D chip (rad-hard/DMILL) chip. The FE-D chips were only received by ATLAS one month ago and so the noise and threshold spread for this chip are in the process of being measured. It is expected that the FE-D will perform well. As a backup plan the ATLAS FE-B (radsoft/HP) chip will

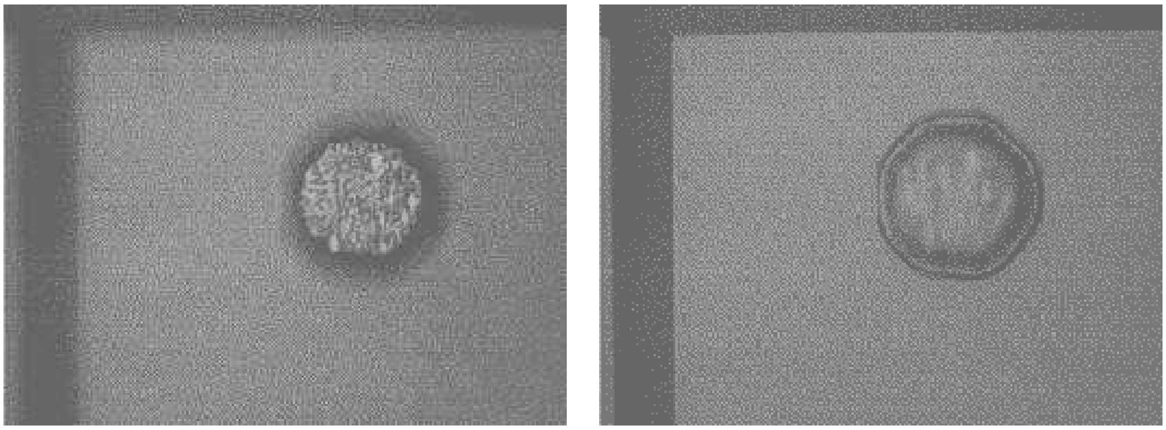

Figure 26: Photograph of a single bump of a CMS diamond pixel detector.

be available. This chip is not optimum for diamond pixel detectors due to its relatively high minimum threshold and relatively high noise spread. The advantage of this chip is that it has been thoroughly tested by the ATLAS pixel group and its properties are understood.

For indium bump-bonding IZM working together with the Bonn group will deposit the bumps and perform the flip-chiping. The practice part was used to qualify the IZM process. At present the diamond detector has undergone a through review by IZM and they have made suggestions for improvement on our end to make their work easier. The holders for the small parts have been fabricated and indium bumps are presently being deposited. We expect the final devices back in early January 2000 when they will be mounted on hybrids and wirebonded at Bonn. We expect to test the completed devices at CERN in early 2000.

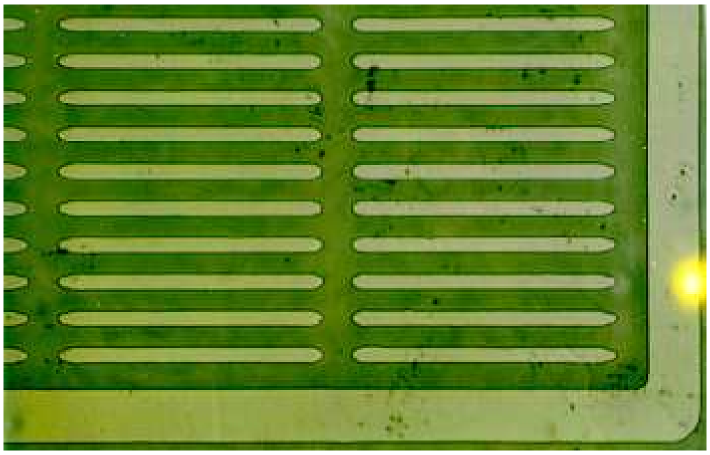

Figure 27: Photograph of a corner of a diamond detector with the ATLAS contact pattern.

6 Diamond Solid State Characterization and Growth

Work related to diamond solid state characterizations and growth is summarized below.

6.1 Work at LETI, CEA Saclay

LETI is involved in the growth of diamond films and in the fabrication and characterization of diamond radiation detectors. Fundamental studies carried out at LETI give insight into the interplay of diamond growth parameters with electronic properties of the diamond. High quality diamond materials are produced by the microwave chemical vapour deposition (MWCVD) technique. Growth reactors which operate at 2.45 GHz are used for the synthesis of diamond films on 5 cm diameter silicon substrates. The study concentrates on the growth of relatively thin films (< 200 μm) which is thinner than diamond samples commonly used by the collaboration. It was found that the electrical characteristics of the films depend on the growth paramters, namely the gas mixture (CH_4, H_2, O_2, N_2) and pressure (from 50 mbar to 150 mbar), the substrate temperature (from $T = 700$ °C to 1000 °C) and the microwave power (from $P = 1.5$ kW to 5 kW). The results show that amongst the growth parameters, the gas mixture has the strongest impact on the charge collected. For fixed deposition parameters ($P = 1.5$ kW, $T = 850$°C and for a film thickness of 20 μm) a decrease of the CH_4 concentration (diluted in H_2) from 3 % to 0.5 % is found to result in a five fold improvement of the mean charge collected. The improvement was directly correlated to the reduction of the width of the diamond RAMAN peak at 1332 cm^{-2} and the amount of non-diamond sp^2 to diamond sp^3 atomic bonds.

6.2 Study of Trap Levels at University of Florence

The present activity of the University and INFN of Florence is related to the characterization of trapping processes in diamond aimed to study trap levels that can affect the collection efficiency in irradiated and non-irradiated samples. The main characterization techniques used are the Thermal Stimulated Currents (TSC), the Photo Induced Conductivity Transient Spectroscopy (PICTS) and the Photo-Luminescence spectroscopy. In TSC the charge trapped in lattice defects during irradiation with electrons from a linear accelerator or photons from a UV Xe source is released thermally by means of a heating scan yielding current signals at different temperatures (in the range from 40 K to 600 K). This technique provides a sensitive method to evaluate the activation energy, capture cross section and defect concentration involved in transport processes. The same information is delivered by PICTS which analyses current transients due to pulsed excitations. The data from TSC and PICTS can be cross-combined to give a reliable determination of the trap parameters. The main defects observed in non-irradiated CVD diamond samples are characterized by energy levels ranging from 0.4 eV to 1.4 eV [10]. Related defect concentrations up to 10^{18}/cm^2 have been estimated. The same study has been performed after irradiation with neutron fluences up to 10^{15}/cm^2 (1 MeV equivalent). The charge collection distance (ccd) of the irradiated samples has also been measured at NIKHEF Amsterdam to correlate the change of the ccd with the radiation-induced defect distribution. A decrease of a 40 % in the ccd has been observed after the highest fluence of irradiation. The activation energies and capture cross-sections of the main native defects do not change significantly after irradiation, while a definite decrease in the TSC signal is observed. This effect depends only in part on the decrease in the ccd, as the TSC signal decreases about one order of magnitude after the highest irradiation. To investigate a wider range of energies and locate deeper defects involved in the collection efficiency, PL measurements are in progress by means of UV laser excitation above bandgap. The group in Florence has also developed a proprietary CVD reactor to prepare diamond samples with known deposition parameters in order to relate the parameters with the crystalline quality and the transport properties. The method is a plasma glow discharge CVD able to grow samples of 1 cm diameter and hundreds of micrometers thick using a mixture of about 1 %

methane in hydrogen. The same characterizations as for the commercial CVD samples are performed.

6.3 INFN Milano

The Milano group is highly interested in CVD diamond detector development mainly in connection with the BTeV experiment at FNAL. The inner tracking of BTeV has to operate in a region very close to the beam pipe and the diamond option can provide a much longer lifetime of the detectors as compared to silicon. The Milano group has joined the RD42 collaboration in 1998 and is involved in 3 main activities: 1. Characterization of the Diamond detector as tracking device, 2. Montecarlo simulation of the charge collection, 3. Design of low-noise front end preamplifier for low capacitance. The simulation is capable to reproduce the charge collection measurements at various bias voltages. The group of Politecnico di Milano has designed a very low power ($< 300\ \mu$W) analog preamplifier/shaper/driver to be coupled to a 1 pF detector and producing a semi-Gaussian output pulse of less than 20 ns peaking time [11]. The circuit, requiring a single supply at 1.6 V, has been tested in laboratory and demonstrated optimum performance. A multichannel version of the same circuit is under realization. The activity for the year 2000 will be devoted to laboratory test and beam tests of the multichannel chip and to the production of a tracking device (strip and/or pixel) with the new electronics. A study will be also done to design a precision low power comparator to be cascaded to the current chip to provide digital information of the occurrance of the event.

6.4 Application of CVD Diamond at GSI, Darmstadt

The suitability of CVD-diamond layers to be used as heavy-ion detectors in fixed-target measurements with high-luminosity beams is established. Different heavy projectiles from ^{12}C to ^{238}U ions are used in an energy range between 120 keV/amu and 2 GeV/amu. The only disadvantage found is a reduced pulse-height resolution of the detectors of about 70 %. Nevertheless, the results obtained open a wide field of heavy ion timing applications in accelerator beam diagnostics, in nuclear physics experiments and in the tumor therapy with carbon ions. The key to all applications is the unique narrow single-particle pulse, amplified and processed with low-noise broadband electronics (50 Ω, $f > 2$ GHz). By matching the strip capacitance a single-pulse FWHM below 1 ns can be achieved leading to a count-rate capability above 10^8 Hz per detector channel. An intrinsic time resolution below 50 ps is common in diamond detectors. In the last year the diamond work at GSI concentrated on the development and design of further detectors to be applied in different domains.

Several devices are already in operation as an essential part of nuclear physics experiments or of beam diagnostics applications including a *start/veto* pair of 25×15 mm^2 diamond strip detectors in the HADES experiment and very thin beam/bunch shape detectors deployed along the along the GSI synchrotron. CVD diamond detectors are also used to perform absolute dose measurements in tumor-therapy with carbon ions at GSI. The CVD sensors employed here are novel large-area position-sensitive dosimeters capable of monitoring doses in excess of 10^8 ions/s. The heavy ion fluence which starts damaging CVD-diamond is still not known. Detectors irradiated with 5×10^{10} per cm^2 of ^{238}U ions at 1 GeV/amu still show improving performance. At this fluence the radiation hardness of CVD sensors is three orders of magnitude better than competitive devices such as silicon diodes or plastic scintillators.

We will continue with the development of diamond detector in each of the areas mentioned above. The main focus of this work will be on tumor therapy detectors in the coming year. We continue to benefit from a fruitful collaboration with RD42 as well as with diamond manufacturers.

7 Proposed Research Program for 2000

7.1 Testbeam Plans for 2000

In order to quantify the developments that occur in diamond material the RD42 program requires testbeam time. As stated earlier the main goals we hope to achieve in the year 2000 are :

- to test LHC pixel detectors with ATLAS and CMS electronics,
- to finalize the geometry and metallization of LHC pixel sensors,
- to finalize the LHC specific electronics performance for diamond trackers.
- to quantify with respect to material properties as a function of the position:
  signal charge, width of the signal distribution, mean residual and spatial resolution.

In addition testbeam time will be used to test new material with strip detector patterns to qualify it for use as pixel detectors. The completion of the RD42 program will be compromised without testbeam time. In order to complete this program we propose 3 testbeam periods with pions of one week each at either the PS or SPS with a momentum of 7 GeV/c or above.

7.2 Plans for Future Work with Diamond Manufacturer's

While we have undertaken a number of additional studies of the properties of the highest quality CVD diamond material that has been developed as part of the RD42 program over the last 5 years we are now in a position to move towards the development of full scale prototype diamond detectors. We intend to move towards proposals that involve the use of this material in high radiation regions of LHC (and other) experiments where its tolerance to dose should make it an ideal alternative to silicon.

To this end we are organising a meeting where prospective particle physicists, not necessarily those involved in the RD42 programme, can meet with diamond manufacturer's to discuss the current state of the art in CVD material and the feasibility of developing material for particular applications in particle physics. It is anticipated that this meeting will take place at CERN on March 6, 2000.

8 Responsibilities and Funding for 2000

What follows is a breakdown of the areas of research that will be pursued at the different institutes (Table 1) involved in the project, a budget for the work to be carried out (Table 2) and sources of funding expected for the project (Table 3).

8.1 Requests from CERN Infrastructure

It is anticipated in addition to the funding needed to purchase diamond samples and develop radiation hard low noise electronics, that the following requests will be made on the CERN infra-structure:

- three 7-day testbeam running periods per year for the duration of the project;
- maintain the present 20 m^2 of laboratory space for test setups, detector preparation and electronics development;
- maintain the present office space for full time residents and visiting members of our collaboration;

8.2 Research Responsibilities

	Diamond Characterization	Meeting with Companies	Radiation Hardness	Detector Design LHC	Detector Design Heavy Ion	Detector Design other	Rad.Hard Electronics	Data Analysis	Material Studies	Diamond Growths
Vienna	x		x					x		
GSI	x				x				x	
LETI/CEA	x								x	x
Univ. Florence	x								x	x
LEPSI/CNRS	x		x	x			x			
Rutgers	x		x					x		
CERN		x	x	x			x		x	
CPPM							x			
LEPES									x	
NIKHEF	x		x					x		
Univ. Torino	x								x	
OSU	x	x	x					x	x	
Bristol			x							
Hamburg	x								x	
Pavia							x			
INFN Milano	x					x	x	x	x	
FNAL								x		
CMU	x					x			x	
UTO	x	x						x		
IIT						x				

Table 1: Research interests of groups involved in RD42.

8.3 Funding Request

Item Budget	(2000)
Raw Diamond Material	250
Detector Fabrication	50
Slow Low Noise Electronics	15
Fast Radiation Hard Electronics	-
Auxiliary Electronics	10
Offline Computing	-
Travel	75
Totals	400

Table 2: Estimated Budget (in kCHF).

Institute (Anticipated Funding)	(2000)
CERN	50
CPPM	20
Florence	10
GSI	5
LENS	5
LEPES	5
LEPSI	15
Milano	25
NIKHEF	20
Toronto	20
U.K.	5
U.S.A. (groups in total)	150
Vienna	20
Totals	400

Table 3: Funds (in kCHF) used for RD42 work subject to approval of national funding agencies.

9 Publications and Talks given by RD42

9.1 Talks since 1997

1. VHLC Workshop, FNAL 1997
2. Elba 97, Elba 1997
3. 2nd Int. Conf. on CP Violation, Honolullu 1997
4. Vertex 97, Rio de Janeiro 1997
5. 5th Symp. on Diamond Materials, Paris 1997
6. EPS 97, Jerusalem 1997
7. 3rd Int. Meeting on Front-End Electronics for High Resolution Tracking Detectors, Taos 1997
8. 3rd Int. (Hiroshima) Symposium on the Development and Application of Semiconductor Tracking Detectors, Melbourne 1997
9. Vienna Wire Chamber Conference, Vienna 1998
10. 2nd Int. Conf. on Radiation Effects in Semiconductor Materials, Detectors and Devices, Florence, 1998 (2 talks)
11. Pixel 98, FNAL 1998 (2 talks)
12. VERTEX 98, Santorini 1998
13. 6th Int. Conf. on New Diamond Sci. and Techn., Pretoria 1998
14. 6th Int. Workshop on GaAs and Related Compounds, Prague 1998
15. 6th Int. Conf. on Advanced Technology and Particle Physics, Como 1998 (two talks)
16. VERTEX 99, Texl, Netherlands 1999
17. 10th European Conf. on Diamond and Related Materials, DIAMOND 99, Prague 1999
18. 7th Int. Conf. for Colliding Beam Physics, INSTR 99, Hamamatsu 1999

9.2 Publications since 1998

1. W. Trischuk *et al.* (RD42 Collaboration), "Semiconductor Trackers for Future Particle Physics Detectors", in Proc. of Vienna Wire Chamber Conference, Vienna, (1998).

2. E. Berdermann *et al.*, "Diamond Detectors for Heavy Ion Measurements at GSI Darmstadt", Nucl. Instr. Meth. **B61** (1998) 399.

3. P. Weilhammer *et al.*(RD42 Collaboration), "Recent Results on CVD Diamond Radiation Sensors", Nucl. Instr. and Meth. **A409** 264 (1998) 264

4. W. Adam *et al.* (RD42 Collaboration), "CVD Diamond Microstrip Detectors", in Proc. of 2$^{\text{nd}}$ Int. Conf. Radiation Effects Semiconductor Mat., Detectors and Devices, Florence (1998).

5. W. Trischuk *et al.* (RD42 Collaboration), "Bump Bonded Pixel Detectors on CVD Diamond from RD42", in Proc. of Int. Pixel Workshop, FNAL, (1998).

6. R. Stone *et al.* (RD42 Collaboration), "Radiation Hardness of CVD Diamond Detectors", in Proc. of Int. Pixel Workshop, FNAL, (1998).

7. D. Meier *et al.* (RD42 Collaboration), "Proton Irradiation of CVD Diamond Detectors for High Luminosity Experiments at the LHC", CERN-EP/98-79, Nucl. Instr. Meth. **A426** (1999) 173.

8. R. Wedenig *et al.* (RD42 Collaboration), "CVD Diamond Pixel Detectors for LHC Experiments" Nucl. Phys. **B78** (1999) 497-504.

9. E. Berdermann *et al.*, "First Applications of CVD-Diamond Detectors in Heavy-Ion Experiments", Nucl. Phys. (Proc. Suppl.) **B78** (1999) 533-539.

10. F. Hartjes *et al.* (RD42 Collaboration), "Parametrisation of radiation effects on CVD diamond for proton irradiation", Nucl. Phys. **B78** (1999) 675.

11. S. Schnetzer *et al.* (RD42 Collaboration), IEEE Trans. Nucl. Sci. **46** (1999) 3.

12. W. Adam *et al.* (RD42 Collaboration), "Review of the Development of Diamond Radiation Sensors", Nucl. Instr. Meth. **A434** (1999) 131-145.

13. M. Friedl *et al.* (RD42 Collaboration), "CVD Diamond Detectors for Ionizing Radiation" Nucl. Instr. Meth. **A435** (1999) 194.

14. W. Adam *et al.* (RD42 Collaboration), "The First Bump-Bonded Pixel Detectors on CVD Diamond", Nucl. Instr. Meth. **A436** (1999) 326-335.

15. F. Hartjes *et al.* (RD42 Collaboration), "Amplitude Distribution and Radiation Tolerance of CVD Diamond" Proc. of VERTEX 99 (accepted).

References

[1] De Beers Industrial Diamond Division (UK) Ltd. Charters, Sunninghill, Ascot, Berkshire, SL5 9PX England.

[2] "Large Hadron Collider Committee, Minutes of the 36. Meeting". http://www.cern.ch/Committees/LHCC/LHCC36.html, (Sep. 1998).

[3] W. Adam *et al.* (RD42-Collaboration). "Development of Diamond Tracking Detectors for High Luminosity Experiments at the LHC". Status Report/RD42, CERN, (June 1998). LHCC 98-20, www.cern.ch/RD42.

[4] C. Colledani *et al.* "A Submicron Precision Silicon Telescope for Beam Test Purposes". *Nucl. Instr. Meth.*, **A372** (1997) 3.

[5] D. Meier. *"CVD Diamond Sensors for Particle Detection and Tracking"*. PhD thesis, University of Heidelberg and CERN, atlasinfo.cern.ch/Atlas/documentation/thesis/thesis.html, (1999).

[6] Integrated Detector and Electronics (IDE) AS. "The VA Circuits". http://www.ideas.no. Pb.315, Veritasveien 9, N-1322 H15vik, Norway, Tel: ++47-6755-1818.

[7] W. Adam *et al.* (RD42-Collaboration). "Development of Diamond Tracking Detectors for High Luminosity Experiments at the LHC". Status Report/RD42, CERN, (Jan. 1997). LHCC 97-3.

[8] C. Posch. *"Analogue Readout for the ATLAS Semiconductor Tracker"*. PhD thesis, Vienna University of Technology and CERN, (1999).

[9] W. Dabrowski *et al.* "Design and Performance of the ABCD Chip for the Binary Readout of Silicon Strip Detectors in the ATLAS Semiconductor Tracker". *Proc. of the IEEE Trans. Nucl. Sci. Symp., Paper N14-42, Seattle*, (1999).

[10] E. Borchi *et al.* "Photo-induced Current Spectroscopy in Undoped CVD Diamond Films". In *Fall Meeting Conf. Proc., Massachusetts*. Mat. Res. Soc., (1999).

[11] G. Bertuccio *et al.* "Low Power Bipolar Front End Circuit for VLSI Detector Readout". *Nucl. Instr. Meth.*, **A412** (1998).